NANO LETTERS

Letter

pubs.acs.org/NanoLett

Ultrabroadband Photonic Structures To Achieve High-Performance Daytime Radiative Cooling

Eden Rephaeli,*[,†,§] Aaswath Raman,*[,†,§] and Shanhui Fan*[,‡]

[†]Department of Applied Physics and [‡]Department of Electrical Engineering, Stanford University, Stanford, California 94305, United States

ABSTRACT: If properly designed, terrestrial structures can passively cool themselves through radiative emission of heat to outer space. For the first time, we present a metal-dielectric photonic structure capable of radiative cooling in daytime outdoor conditions. The structure behaves as a broadband mirror for solar light, while simultaneously emitting strongly in the mid-IR within the atmospheric transparency window, achieving a net cooling power in excess of 100 W/m^2 at ambient temperature. This cooling persists in the presence of significant convective/conductive heat exchange and nonideal atmospheric conditions.

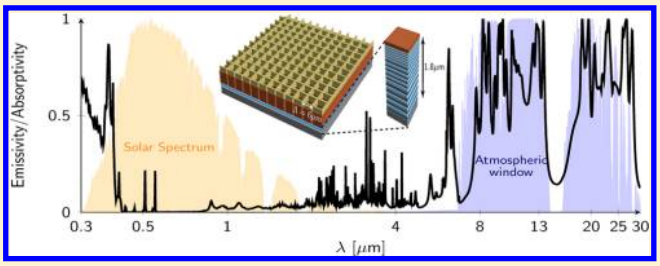

KEYWORDS: *Radiative cooling, thermal radiation, broadband solar mirror, phonon-polariton, selective emission*

The Earth's atmosphere has a transparency window for electromagnetic waves between 8−13 μm that coincides with peak thermal radiation wavelengths at typical ambient temperatures. By exploiting this window one can cool a body on the Earth's surface by radiating its heat away into cold outer space. This radiative cooling mechanism is attractive to energy efficiency improvement efforts because it provides a purely passive cooling strategy for terrestrial structures without the need for any energy inputs.

While nighttime radiative cooling has been extensively studied,[1−7] the peak demand for cooling occurs during the daytime. Thus, it is of great importance to explore the possibility of daytime radiative cooling. To achieve daytime cooling one needs to design a structure that is simultaneously a broadband mirror for solar light and a strong thermal emitter in the atmospheric transparency window. Previous work in daytime radiative cooling has sought to accomplish this by covering a near-black emitter with a cover foil.[1,8−10] The foil, made of ZnS or ZnSe[9] or polymers and pigments,[10] transmits thermal radiation while reflecting sunlight. However, no actual cooling was demonstrated because the reported solar radiation reflection achieved by these cover foils was no larger than 85%.[9] The limited reflection achieved is partly due to the constraint of simultaneous broadband solar reflection and transparency in the λ = 8−13 μm range on a single material, forcing a compromise between the two.[8]

In recent years, significant progress has been made in the control of thermal emission of light from nanostructured materials.[11−13] Enhancement and suppression of thermal emission of light using photonic structures has been theoretically and experimentally demonstrated in 1D,[14−16] 2D,[17−20] and 3D[11,21−25] photonic crystals, with application to thermophotovoltaics,[21,26,27] solar thermophotovoltaics,[16,28] and waste heat recovery.[29]

Building upon these developments, in this Letter we present for the first time a single compact planar device capable of achieving substantial radiative cooling in the daytime. We also present a theoretical and numerical analysis identifying the critical performance metric targets needed to accomplish daytime radiative cooling. Our design for a daytime radiative cooler, shown in Figure 1a, represents a strong departure from previously published systems. Rather than designing a cover foil that is spatially separated from a black emitter we introduce an integrated thermally selective emitter atop a broadband mirror. Doing so enables us to exploit near-field coupling between material layers, leading to stronger control over emission, absorption, and reflection. Using nanophotonic concepts, our photonic structure is able to strongly suppress solar absorption while enhancing thermal emission in the atmospheric transparency window: an ultrabroadband performance, shown in Figure 1b, capable of achieving a net cooling power exceeding 100 W/m^2 at ambient temperature.

Radiative cooling devices operate at near-ambient temperatures and therefore do not suffer from many of the difficulties associated with other thermal applications of photonic structures that have typically involved high-temperature operation. These difficulties include numerical uncertainty associated with the temperature-dependence of optical properties, material cohesion, small-feature evaporation, and durability that affect other thermal applications.[30] Our approach and design is thus a departure from previous work in using nano- and microphotonic structures for thermal applications.

Received: November 29, 2012
Revised: February 21, 2013
Published: March 5, 2013

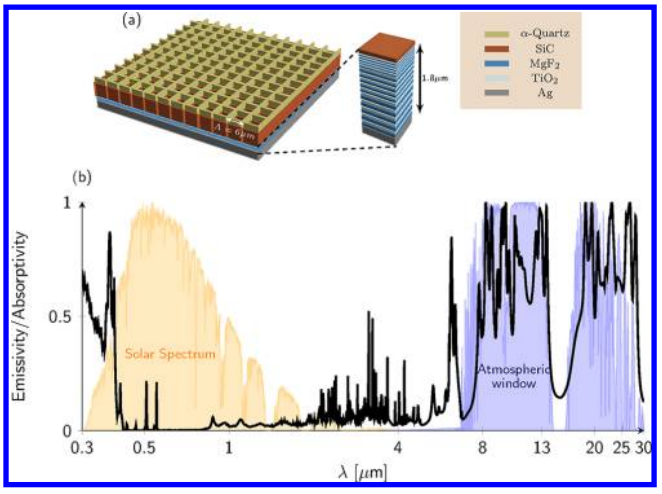

Figure 1. (a) Optimized daytime radiative cooler design that consists of two thermally emitting photonic crystal layers comprised of SiC and quartz, below which lies a broadband solar reflector. The reflector consists of three sets of five bilayers made of MgF_2 and TiO_2 with varying periods on a silver substrate. (b) Emissivity $\varepsilon(\lambda,0)$ of the optimized daytime radiative cooler shown in (a) at normal incidence (black) with the scaled AM1.5 solar spectrum (yellow) and atmospheric transmittance $t(\lambda)$ (blue) plotted for reference. The structure has minimal absorption throughout the solar spectrum and has very strongly selective emission in the atmospheric transparency window, as is desirable and necessary for a high-performance daytime radiative cooler.

To begin our analysis, we consider a photonic structure at temperature T whose radiative properties are described by a spectral and angular emissivity $\varepsilon(\lambda,\theta)$. The structure is exposed to a clear sky subject to solar irradiance, and also atmospheric irradiance corresponding to an ambient temperature T_{amb}. The net cooling power $P_{net}(T)$ of a structure with area A is given by

$$P_{net}(T) = P_{rad}(T) - P_{atm}(T_{amb}) - P_{sun} \quad (1)$$

where

$$P_{rad}(T) = A \int d\Omega \cos\theta \int_0^\infty d\lambda I_{BB}(T,\lambda)\varepsilon(\lambda,\theta) \quad (2)$$

is the power radiated by the structure

$$P_{atm}(T_{amb}) = A \int d\Omega \cos\theta \int_0^\infty d\lambda I_{BB}(T_{amb},\lambda)\varepsilon(\lambda,\theta)\varepsilon_{atm}(\lambda,\theta) \quad (3)$$

is the absorbed power stemming from atmospheric radiation, and

$$P_{sun} = A \int_0^\infty d\lambda \varepsilon(\lambda,0) I_{AM1.5}(\lambda) \quad (4)$$

is the incident solar power absorbed by the structure. Here $\int d\Omega = 2\pi \int_0^{\pi/2} d\theta \sin\theta$ is the angular integral over a hemisphere. $I_{BB}(T,\lambda) = [(2hc^2)/(\lambda^5)][1/(e^{hc/(\lambda k_B T)} - 1)]$ is the spectral radiance of a blackbody[31] at temperature T. In obtaining eq 3 and eq 4 we used Kirchoff's law to replace the structure's absorptivity with its emissivity $\varepsilon(\lambda,\theta)$. The angle-dependent emissivity of the atmosphere is given by[3] $\varepsilon_{atm}(\lambda,\theta) = 1 - t(\lambda)^{1/\cos\theta}$, where $t(\lambda)$ is the atmospheric transmittance in the zenith direction.[32] In eq 4, the solar illumination is represented by $I_{AM1.5}(\lambda)$, the AM1.5 Global Tilt spectrum with an irradiance of 964 W/m^2, which represents the average solar conditions of the continental U.S. We assume the structure is

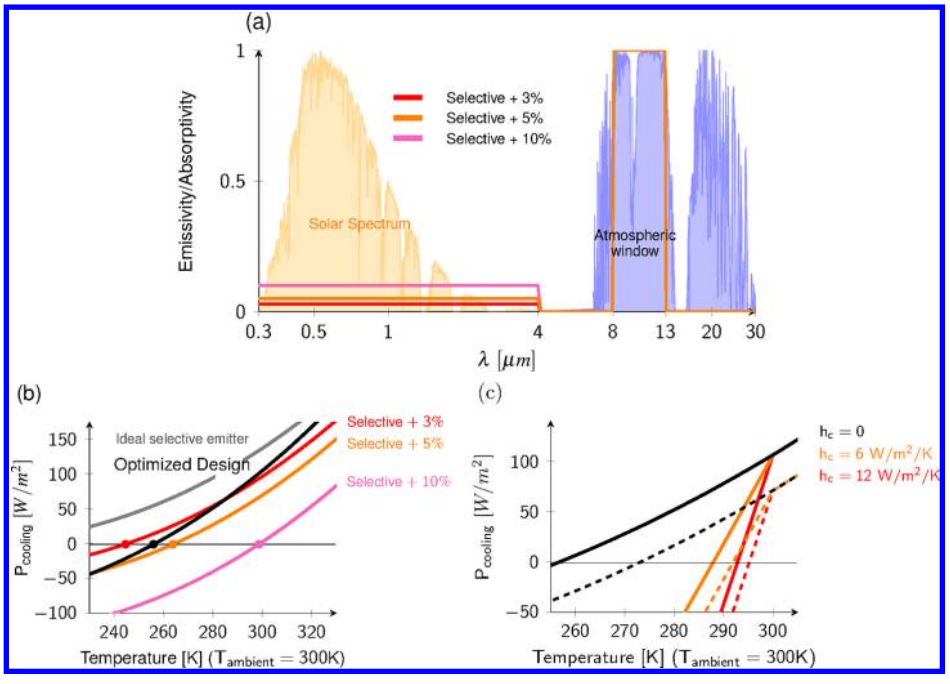

Figure 2. (a) Emissivity (Absorptivity) spectrum $\varepsilon(\lambda,0)$ of selective emitters with 3,5, or 10% absorption of AM 1.5 solar spectrum (shaded yellow). The atmospheric transmittance $t(\lambda)$ is plotted in shaded blue. (b) Net cooling power P_{net} versus radiative cooler temperature for selective emitters shown in (a). The equilibrium temperatures T_{eq} for these emitters, noted by the dots along the $P_{net} = 0$ dashed line, are 195 K, 245 K, 265 K, and 300 K, for 0 (ideal) 3, 5, and 10% absorption, respectively. The net cooling power for the optimized design shown in Figure 1a is plotted (in black), achieving an equilibrium temperature of 260 K, and greater cooling power than all but the ideal selective emitter with 0% solar absorption at $T = T_{amb}$. (c) Net cooling power P_{net} of the optimized design versus radiative cooler temperature for the total nonradiative (conductive + convective) heat constant of 0, 6, or 12 W/m^2/K, for the case of either high (solid curves) or low (dashed curves) atmospheric transmittance.

dx.doi.org/10.1021/nl4004283 | Nano Lett. 2013, 13, 1457−1461

facing the sun. Hence the term P_{sun} is devoid of an angular integral, and the structure's emissivity is represented by its value in the zenith direction, $\theta = 0$.

For a cooling structure, there are two important metrics which are indicative of its capacity to cool. P_{net}, the cooling power, is the first metric. To achieve $P_{net} > 0$ at a given T and T_{amb}, in eq 1 the emissivity $\varepsilon(\lambda,\theta)$ must be high within the atmospheric transparency window and absorptivity must be low at wavelengths in which the atmosphere is emissive. Thus in general, for both daytime and nighttime cooling, the structure must emit selectively only where the atmospheric transmittance $t(\lambda)$ is significant, that is, the transparency window from 8 to 13 μm. Emission of light from the structure at wavelengths of low atmospheric transmittance entails absorption of atmospheric radiation, thereby increasing P_{atm}. This need for selective thermal emission motivates our interest in using phonon-polariton materials in the structure shown in Figure 1a. For daytime cooling, in addition, the structure must minimize P_{sun}.

The other cooling metric is T_{eq}, the temperature at which $P_{net} = 0$ in eq 1. A radiative cooler with T_{eq} below the ambient temperature would thus cool an attached structure, via heat conduction, to a temperature below ambient over time and perform the system-wide cooling desired. Thus, in evaluating our radiative cooler design one of our key goals will be to numerically demonstrate an integrated cooling structure which has an equilibrium temperature T_{eq} below the ambient T_{amb} under peak daylight conditions. This has never been done before in a compact planar structure.

Using the theory described above, we first evaluate the ideal situation. In the absence of sunlight, for a radiative cooler at temperature T approximately equal or larger than T_{amb}, the greatest cooling power P_{net} is achieved by a blackbody emitter. However, P_{net} of a blackbody emitter drops sharply as T falls below T_{amb}. It follows that the lowest possible T_{eq} is attained by an ideal selective emitter with 'tophat' emissivity $\varepsilon(\lambda,\theta) = 1$ for $8\ \mu\text{m} < \lambda < 13\ \mu\text{m}$, and $\varepsilon(\lambda,\theta) = 0$ elsewhere.[3] The emissivity of such an ideal selective emitter is shown in Figure 2a. The requirement for the emissivity to go to zero everywhere outside the 8−13 μm wavelength range is a formal one, and at night need only be satisfied in the vicinity of the atmospheric transparency window.

During the day, however, the requirement of zero emissivity outside the atmospheric window is quite formidable and minimizing the absorption of solar light becomes an overriding imperative in order to achieve radiative cooling. To demonstrate this we plot $P_{net}(T)$ in Figure 2b, where $T_{amb} = 300$ K, for an ideal radiative cooler with the selective emissivity described above. The performance of the cooler degrades as it absorbs increasing fractions of the incident solar light, as shown in Figure 2a. The ideal daytime radiative cooler (0% solar absorption) can reach a very low $T_{eq} = 195$ K, but with just 10% solar absorption T_{eq} shoots up to nearly the ambient temperature, such that no meaningful cooling is achieved.

As can also be seen from comparing the curves in Figure 2b, absorbing even a small fraction of solar radiation has direct and significant implications on the achievable cooling powers of these radiative coolers. The 10% solar spectrum absorption yields a meager cooling power of 3 W/m^2 at $T = T_{amb}$, as opposed to 3% solar absorption that leads to a practically meaningful cooling power of 100 W/m^2. These results indicate the importance of suppressing solar absorption maximally. This in turn points to a key aspect of our design that is novel: we use dielectric, instead of metallic, reflective substrates in the radiative cooler to achieve well below 10% solar absorption. Finally, we note that Figure 2b demonstrates the great potential of daytime radiative cooling with cooling powers in excess of 150 W/m^2 theoretically possible when solar radiation is maximally reflected.

At a system level, the radiative cooler would receive heat conducted from the building or device it is cooling at a rate $P_{conducted}$. If $P_{conducted} \ll P_{net}(T_{bldg})$, where T_{bldg} is the temperature of the building, then the building provides a negligible amount of heat and the radiative cooler will reach a temperature close to T_{eq}. However, as $P_{conducted}$ increases, so does the relative importance of the metric $P_{net}(T)$. Thus, depending on the specific application and location, the relative importance of either one of the two performance metrics will change. For example, P_{net} is thought to be a more important metric in warm tropical climates.[33] The key point here is that once solar absorption is brought to a low enough level, as we accomplish with our design, one can further customize the design to either give preference to, or balance the requirements for achieving, a low T_{eq} or a high P_{net}.

On the basis of the theoretical discussion above, we now present a compact planar photonic structure that minimizes absorbed solar radiation, P_{sun}, and atmospheric radiation, P_{atm}, while maximizing its emitted radiative power P_{rad}. The structure, shown in Figure 1a, consists of two components: a two-layer 2D photonic crystal employing phonon−polariton modes to maximize emissivity in the atmospheric transparency window and a chirped 1D photonic crystal reflector designed to minimize absorbed solar radiation and lying beneath the thermally emitting photonic crystal layers.

As discussed above, maximizing P_{rad} while minimizing P_{atm} involves emitting selectively within the atmospheric transparency window that exists from 8 to 13 μm while minimizing emission above and below these wavelengths. To achieve this level of granular spectral selectivity in thermal emission the 2D periodic photonic design we describe here uses two materials with phonon−polariton resonances in the 8−13 μm range, quartz and SiC. The dielectric function of quartz has a sharp resonance at 9.3 μm whereas that of SiC has a resonance at 12.5 μm, thus providing complementary resonances that cover, and maximize emission selectively in, the atmospheric transparency window. The use of surface phonon−polariton modes to enhance the structure's emissivity further enables broad-angle emission due to their flat energy bands and also keeps the layer thicknesses small. Quartz and SiC are in addition desirable for daylight operation since they are very weak absorbers in the visible and IR, ensuring that a minimal amount of solar power is absorbed in the thermally emitting layers. All optical properties of materials considered are obtained via ellipsometry[34] or through tabulated values.[35]

To take advantage of the phonon−polariton resonances of each material we place quartz and SiC as the top two layers of our cooler and introduce a two-dimensional periodic array of square air holes in both layers to form photonic crystal structures. Extensive optimization for selective thermal emission in the transparency window yields a Quartz layer thickness of 2.5 μm, a SiC layer thickness of 8 μm, a periodicity for both layers of 6 μm, and square air rectangles etched in the quartz and SiC layers of 5.4 μm width.

To minimize the absorbed solar radiation, P_{sun}, we introduce a reflector made of chirped 1D photonic crystals below the two-layer photonic crystal. The 1D photonic crystals consist of alternating layers of TiO_2 (high-index) and MgF_2 (low-index)

dx.doi.org/10.1021/nl4004283 | Nano Lett. 2013, 13, 1457−1461

lying on a silver substrate. To cover the entire solar spectrum we combine three 1D photonic crystal sets, each having five bilayers with different thicknesses, resulting in three overlapping photonic bandgaps.[36] The first set of five bilayers have thicknesses of 25 nm of TiO_2 and 35 nm of MgF_2, the second set 50 nm of TiO_2 and 70 nm MgF_2, and the third set 75 nm of TiO_2 and 105 nm of MgF_2.

We simulate this optimized structure using the rigorous coupled-wave analysis (RCWA) method.[37] To evaluate the structure's effectiveness as a daytime radiative cooler we calculate its absorptivity/emissivity at 2 nm resolution across an ultrabroadband wavelength range from 300 nm (UV) to 30 μm (mid-IR). The resulting absorptivity/emissivity spectrum is shown in Figure 1b, along with overplots of the AM1.5 solar spectrum and the atmospheric transmittance $t(\lambda)$. For wavelengths within the solar spectrum, the structure absorbs minimally with only 3.5% of solar radiation at normal incidence absorbed by the overall structure. The thermally emitting top layers are transparent to solar light, and the chirped 1D photonic crystal reflector is indeed effective at maximizing reflection over the entire solar spectrum. The choice of only five bilayers for each period in the chirped reflector represents a compromise between achieving high reflectance and practicality given the need for less than 5% solar absorption identified in the previous section.

Within the atmospheric transparency window the structure acts as a very strong and selective emitter. Many sharp peaks can be observed in the spectrum in addition to some notable dips due to the material properties of SiC and quartz. The structure's emissivity is strongly suppressed outside the transparency window. We also note here many emissivity peaks in the 20−30 μm range. These peaks are actually beneficial due to the presence of a secondary atmospheric transparency window between 20 and 25 μm that is also highlighted in Figure 1b.

To elucidate the source of the emissivity in the transparency window across all angles we calculate the folded-band structure for bulk SiC and quartz assuming a period of 6 μm in Figure 3a. We then use emissivity data for the structure at various polar angles of incidence to plot the emissivity versus parallel wave vector $\mathbf{k}_{\|}$ in Figure 3b. Many of the bands calculated in Figure 3a, in particular the flat phonon-polariton bands[38] for both quartz and SiC, are clearly visible in Figure 3b. Moreover, we observe the contribution of each material's resonances to the overall emissivity of the photonic crystal.

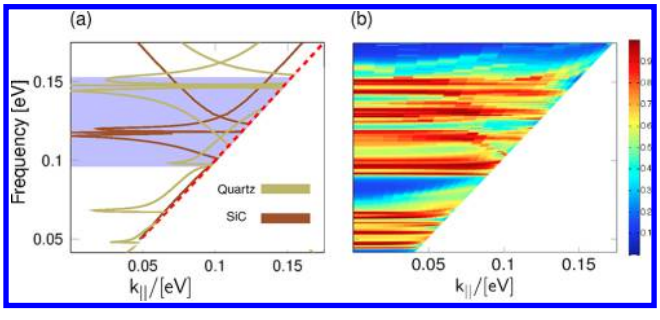

Figure 3. (a) Folded band structure of semi-infinite slabs of SiC and α−Quartz above the lightline with a 6 μm period. Light-line in dashed red. Flat bands corresponding to the surface modes of SiC and quartz are clearly visible near their surface phonon−polariton frequencies. (b) Absorptivity/emissivity versus parallel wavenumber $\mathbf{k}_{\|}$. We observe strong emission to large angles (large $\mathbf{k}_{\|}$) corresponding to the surface modes of SiC and quartz, a highly desirable feature since the power radiated $P_{cooling}$ and T_{eq} are hemispherically integrated quantities.

In Figure 2b, we plot $P_{net}(T)$ given T_{amb} = 300 K for our structure, calculated via hemispheric integration of the structure's emissivity, shown along with the previously plotted $P_{net}(T)$ for a selective emitter with added 3, 5, and 10% solar absorption. Our designed structure is seen to have a remarkably low daytime equilibrium temperature of 260 K. It furthermore has a cooling power of 105 W/m^2 at T_{amb}. We note that $P_{net}(T_{amb})$ surpasses the highest achievable cooling rate of the ideal selective emitter with 3% solar absorption owing to our structure's broader emission spectrum. Thus, the design strikes a good balance between obtaining a large P_{net} at ambient temperature, and achieving a low T_{eq}.

The key technical issues that can hamper radiative cooling are nonradiative heat transport and nonideal atmospheric conditions leading to diminished transmittance. The effects of conductive and/or convective heat exchange is accounted for by adding a term $P_{cond+conv} = h_c(T_{amb} - T)$ in eq 1 for $T < T_{amb}$. Placing the structure on polystyrene results in a conductive heat coefficient value of h_{cond} = 0.3 W/m^2/K. The presence of 1 m/s and 3 m/s wind speed would result in a combined nonradiative heat coefficient of $h_c = h_{cond} + h_{conv}$ of ≈6 and ≈12 W/m^2/K, respectively.[9] The primary phenomenon causing diminished atmospheric transmission is continuum absorption. This absorption is dependent on the amount of water vapor in the atmosphere, the air temperature, and the dewpoint temperature[39] but can be captured by an effective atmospheric transmittance, $t(\lambda)$ in eq 3. In ref 4, an effective transmittance plateau of $t(\lambda) \approx 0.6$ between 8−13 μm is given as an accurate representation of three locations in the U.S. In Figure 2c, we plot $P_{net}(T)$ of our structure given T_{amb} = 300 K for various values of h_c and both high[32] and low[4] (an average of 0.6) atmospheric transmittance. In both cases, significant cooling can still be achieved even for a value of h_c = 12 W/m^2/K in which case the structure reaches an equilibrium temperature of T = 293 K and T = 296 K with cooling powers of 105 and 70 W/m^2 at ambient, respectively. Thus, even in the presence of realistic conductive heat exchange and moderate wind-induced convection, significant cooling remains possible. Moreover, encapsulating our structure with a cover can completely eliminate wind convection. Because our structure already strongly reflects solar light, the demands on the cover material are significantly reduced, in contrast to previously proposed radiative coolers. These previously proposed coolers relied on the cover foil to both transmit in the 8−13 μm wavelength range and reflect solar light, whereas for our design it need merely be transparent in the window. From this discussion, it is evident that using photonic structures in a radiative cooler setup not only allows daytime cooling to occur, but also leads to a more robust cooling performance, relative to previously published systems, in the face of nonidealities.

In considering the systemwide impact of the daytime radiative coolers we have designed, we first place the cooling powers achieved in context. Consider for example that solar panels at 10% efficiency will generate roughly 100 W/m^2 at peak. The passive daytime radiative coolers proposed here can thus be thought of as solar panel substitutes by reducing the demand on a rooftop solar system from air conditioning systems. A recent study from NREL found a peak cooling load of approximately 6 kW in Chicago and Orlando for canonical 2233 ft^2 one-story homes in the summer.[40] Assuming the radiative cooler is operating at its peak cooling rate, then for

dx.doi.org/10.1021/nl4004283 | Nano Lett. 2013, 13, 1457−1461

just 20 m^2 of daytime radiative cooler on the rooftop (10% of a total of 200 m^2 available rooftop space), one can offset 35% of the house's air conditioning needs during the hottest hours of the day.

Finally, we note that the techniques needed to fabricate the structures discussed here are well validated and understood, and within the scope of current technology. Recent work on roll-to-roll nanoimprint lithography has already successfully produced nanoscale patterns on large areas[41] and may be of particular relevance to producing large area samples of such photonic structures. Furthermore, the feature sizes of our design are amenable to conventional wafer-scale photolithography and processing steps, making large scale production possible with existing facilities.

In conclusion, we have numerically demonstrated for the first time a macroscopically planar structure capable of achieving radiative cooling in the daytime, even in the presence of realistic nonradiative heat transfer. In contrast to previous approaches to radiative cooling, we have used concepts from nanophotonics to design a dielectric reflector, which minimizes solar absorption, and a two-layer 2D photonic crystal of SiC and quartz, which selectively emits thermal radiation in the atmospheric transparency window. These two functionalities are combined into a single device that achieves the ultrabroadband performance needed to radiatively cool in the daytime. Currently, applications of thermal light sources are being explored mainly in the field of thermophotovoltaic power conversion but the demands of high-operating temperatures inevitably leads to nano- and microscopic material degradation, presenting a formidable challenge. In our work, we have presented another application of thermal light emission from microstructured materials, radiative cooling. In contrast to previous applications, using thermal light emission to cool structures does not require high temperature operation. We thus anticipate that radiative cooling will motivate continued interest and research in thermal nanophotonics and metamaterials.

AUTHOR INFORMATION

Corresponding Author

*E-mail: (E.R.) edenr@stanford.edu; (A.R.) aaswath@stanford.edu; (S.F.) shanhui@stanford.edu.

Author Contributions

§These authors contributed equally to this work.

Notes

The authors declare no competing financial interest.

ACKNOWLEDGMENTS

A.R. acknowledges the support of Alberta Scholarship Programs' Sir James Lougheed Award of Distinction.

REFERENCES

(1) Catalanotti, S.; Cuomo, V.; Piro, G.; Ruggi, D.; Silvestrini, V.; Troise, G. *Sol. Energy* **1975**, *17*, 83−89.

(2) Granqvist, C. G.; Hjortsberg, A. *Appl. Phys. Lett.* **1980**, *36*, 139−141.

(3) Granqvist, C. G.; Hjortsberg, A. *J. Appl. Phys.* **1981**, *52*, 4205−4220.

(4) Berdahl, P.; Martin, M.; Sakkal, F. *Int. J. Heat Mass Transfer* **1983**, *26*, 871−880.

(5) Orel, B.; Gunde, M.; Krainer, A. *Sol. Energy* **1993**, *50*, 477−482.

(6) Suryawanshi, C. N.; Lin, C.-T. *ACS Appl. Mater. Interfaces* **2009**, *1*, 1334−1338.

(7) Gentle, A. R.; Smith, G. B. *Nano Lett.* **2010**, *10*, 373−379.

(8) Nilsson, T. M.; Niklasson, G. A.; Granqvist, C. G. *Sol. Energy Mater. Sol. Cells* **1992**, *28*, 175−193.

(9) Nilsson, T. M.; Niklasson, G. A. *Sol. Energy Mater. Sol. Cells* **1995**, *37*, 93−118.

(10) Covering Element screening off the solar radiation for the applications in the refrigeration by radiation. U.S. Patent 4,323,619, 1982.

(11) Lin, S.-Y.; Fleming, J. G.; Chow, E.; Bur, J.; Choi, K. K.; Goldberg, A. *Phys. Rev. B* **2000**, *62*, R2243−R2246.

(12) Schuller, J.; Taubner, T.; Brongersma, M. *Nat. Photonics* **2009**, *3*, 658−661.

(13) Greffet, J. *Nature* **2011**, *478*, 191−192.

(14) Narayanaswamy, A.; Chen, G. *Phys. Rev. B* **2004**, *70*, 125101.

(15) Celanovic, I.; Perreault, D.; Kassakian, J. *Phys. Rev. B* **2005**, *72*, 075127.

(16) Rephaeli, E.; Fan, S. *Opt. Express* **2009**, *17*, 15145−15159.

(17) Le Gall, J.; Olivier, M.; Greffet, J. *Phys. Rev. B* **1997**, *55*, 10105.

(18) Greffet, J.-J.; Carminati, R.; Joulain, K.; Mulet, J.-P.; Mainguy, S.; Chen, Y. *Nature* **2002**, *416*, 61−64.

(19) Luo, C.; Narayanaswamy, A.; Chen, G.; Joannopoulos, J. D. *Phys. Rev. Lett.* **2004**, *93*, 213905.

(20) Chan, D. L. C.; Soljăcíc, M.; Joannopoulos, J. D. *Opt. Express* **2006**, *14*, 8785−8796.

(21) Fleming, J. G.; Lin, S. Y.; El-Kady, I.; Biswas, R.; Ho, K. M. *Nature* **2002**, *417*, 52−55.

(22) Rephaeli, E.; Fan, S. *Appl. Phys. Lett.* **2008**, *92*, 211107.

(23) Arpin, K. A.; Losego, M. D.; Braun, P. V. *Chem. Mater.* **2011**, *23*, 4783−4788.

(24) Wang, M.; Hu, C.; Pu, M.; Huang, C.; Zhao, Z.; Feng, Q.; Luo, X. *Opt. Express* **2011**, *19*, 20642−20649.

(25) Zhang, S.; Li, Y.; Feng, G.; Zhu, B.; Xiao, S.; Zhou, L.; Zhao, L. *Opt. Express* **2011**, *19*, 20462−20467.

(26) Bermel, P.; Ghebrebrhan, M.; Chan, W.; Yeng, Y. X.; Araghchini, M.; Hamam, R.; Marton, C. H.; Jensen, K. F.; Soljačić, M.; Joannopoulos, J. D.; Johnson, S. G.; Celanovic, I. *Opt. Express* **2010**, *18*, A314−A334.

(27) Zhai, X.; Lai, J.; Liang, H.; Chen, S. *J. Appl. Phys.* **2010**, *108*, 074507.

(28) Wu, C.; Neuner, B., III; John, J.; Milder, A.; Zollars, B.; Savoy, S.; Shvets, G. *J. Optics* **2012**, *14*, 024005.

(29) De Zoysa, M.; Asano, T.; Mochizuki, K.; Oskooi, A.; Inoue, T.; Noda, S. *Nat. Photonics* **2012**, *6*, 535−539.

(30) Yeng, Y.; Ghebrebrhan, M.; Bermel, P.; Chan, W.; Joannopoulos, J.; Soljačić, M.; Celanovic, I. *Proc. Natl. Acad. Sci. U.S.A.* **2012**, *109*, 2280−2285.

(31) where c is the speed of light, h is Planck's constant, k_B is the Boltzmann constant, and λ is the wavelength.

(32) IR Transmission Spectra, Gemini Observatory. http://www.gemini.edu/?q=node/10789 (accessed Nov 15, 2012).

(33) Jaffer, A. *Radiative Cooling in Hot Humid Climates*. http://people.csail.mit.edu/jaffer/cool/cool.pdf (accessed Nov 15, 2012).

(34) Hafeli, A. K.; Rephaeli, E.; Fan, S.; Cahill, D. G.; Tiwald, T. E. *J. Appl. Phys.* **2011**, *110*, 043517.

(35) Palik, E. *Handbook of Optical Constants of Solids, Vol.s I, II, and III: Subject Index and Contributor Index*; Academic Press Handbook Series; Elsevier Science & Tech: New York, 1985.

(36) Fink, Y.; Winn, J. N.; Fan, S.; Chen, C.; Michel, J.; Joannopoulos, J. D.; Thomas, E. L. *Science* **1998**, *282*, 1679−1682.

(37) Liu, V.; Fan, S. *Comput. Phys. Commun.* **2012**, *183*, 2233−2244.

(38) Raman, A.; Fan, S. *Phys. Rev. Lett.* **2010**, *104*, 087401.

(39) Berdahl, P.; Fromberg, R. *Solar Energy* **1982**, *29*, 299−314.

(40) Burdick, A. *Strategy Guideline: Accurate Heating and Cooling Load Calculations*; DOE/GO-102011-3304; U.S. Dept. of Energy: Washington, D.C., 2011.

(41) Ahn, S. H.; Guo, L. J. *ACS Nano* **2009**, *3*, 2304−2310.